Feature Selection and Optimal Neural Network Algorithm for the State of Charge Estimation of Lithium-ion Battery for Electric Vehicle Application

M.S. Hossain Lipu*,**‡, M.A. Hannan***, A. Hussain*

*Department of Electrical, Electronic and Systems Engineering, Universiti Kebangsaan Malaysia, Bangi 43600, Selangor, Malaysia
**Department of Electrical and Electronic Engineering, University of Asia pacific, Dhaka 1215, Bangladesh
***Department of Electrical Power Engineering, College of Engineering, Universiti Tenaga Nasional, Kajang 43000, Selangor, Malaysia
(lipu@siswa.ukm.edu.my, hannan@uniten.edu.my, draini@ukm.edu.my)

‡Corresponding Author; M.S. Hossain Lipu, Department of Electrical, Electronic and Systems Engineering, Universiti Kebangsaan Malaysia, Bangi 43600, Selangor, Malaysia; lipu@siswa.ukm.edu.my

Received: 27.03.2017 Accepted:23.09.2017

Abstract- This paper presents the estimation of the state of charge (SOC) for a lithium-ion battery using feature selection and an optimal NN algorithm. Principle component analysis (PCA) is used to select the most influencing features. Out of nine variables, five input variables are selected based on the value of eigenvectors. An optimal neural network (NN) is developed by selecting the hidden layer neurons and learning rate since these parameters are the most critical factors in constructing a NN model. The model is tested and evaluated by using US06 driving cycle at 25°C and 45°C respectively. In order demonstrate the effectiveness and accuracy of the proposed model, a comparative study is performed between proposed NN model and two different NN models (NN1 and NN2). The proposed NN model estimates SOC with lower mean squared error (MSE) and root mean squared error (RMSE) compared to two NN models which proves that the proposed model is competent and robust in estimating SOC. The simulation results show an improvement in proposed NN model accuracy over NN1 and NN2 models in minimizing RMSE by 26% and 22% and MSE by 45% and 39% respectively at 25°C.

Keywords- state of charge; lithium-ion battery; neural network; principle component analysis; data training and testing; mean squared error (MSE); root mean squared error (RMSE)

1. Introduction

With ever rising concerns over climate change, global warming, and energy conservation, research and development on EVs are being actively performed [1]–[4]. EVs have already been widely accepted in the automobile industry and are considered the most promising replacements of gasoline based vehicles in reducing CO_2 emissions [5], [6]. However, the performance of electric vehicles is highly dependent on battery size, cost, safety, battery management system [7]–[9] as well as traction cotrol and heat control [10]. Therefore, a further development is required to enhance the battery performance and efficiency.

There are different categories of batteries are being employed in EVs: Ni-Cd battery, Ni-MH battery, lead-acid battery and lithium-ion battery [11]. Of these, lithium-ion battery has achieved massive popularity due to its lucrative features such as high energy density, high voltage, long life cycle, low self-discharge rate and low pollution [12]–[14]. Due to it its attractive characteristics of the lithium-ion battery, a lot of research and development have already been performed to improve the stability and performance [15]. However, the lithium-ion battery still suffers from high initial cost and its unstable operation in battery charging and discharging [16]. Even though the lithium-ion battery has some drawbacks, the market progress has been growing gradually and is likely to continue its growth in future [17].

The SOC in one of the critical parameters to signify the current and remaining performance of a battery. Battery SOC describes how the much charge is available inside a battery to drive an electric vehicle. Nevertheless, Estimating battery SOC accurately is a challenging task and it cannot be computed directly because the lithium-ion battery has non-linear, time-varying characteristics and complex electrochemical reactions [18]. Furthermore, lithium-ion battery is very sensitive to some internal and external factors [19]–[21]. Battery SOC can be calculated in many ways. For instance, ampere-hour method uses current integration to

estimate SOC which is the easiest method and can be implemented with low power consumption. However, the method suffers from determining the initial value of SOC which causes a cumulative effect [22]. Open circuit voltage (OCV) is another commonly used method which estimates SOC with high accuracy. However, OCV needs long rest time to reach steady state condition [23]. Kalman filter (KF) has been the most widely used method to estimate battery state. Nevertheless, the model has high mathematical computation and is extremely vulnerable to aging, temperature and external disturbances [24]. Fuzzy logic (FL) is an intelligent algorithm that estimates SOC considering aging, temperature, and noises. Nonetheless, the method requires lots of computation and a huge amount of training data as well as costly processing unit [25]–[27]. Support vector machine (SVM) has satisfactory performance in battery nonlinear and high dimension model. The method has benefits of estimating SOC quickly and accurately. However, highly complex computation makes the process difficult to be executed in the BMS [28].

To overcome these shortcomings, an optimal neural network (NN) algorithm is proposed to estimate the SOC of a lithium-ion battery for an electric vehicle application. This paper uses the feedforward backpropagation (BP) NN which updates the weights and biases of each hidden layer to minimize error. Firstly, an optimal number of input variables is selected out of many variables using PCA which has a significant impact in improving accuracy. Secondly, a number of hidden layer neurons and learning rate are optimized to reduce the MSE and RMSE between actual SOC and estimated SOC.

The paper is arranged as follows. Section two describes the steps and explanation of input data selection based on PCA. The data collection method is presented in section three. Section four describes data normalization and preprocessing. The explanation of NN structure is presented in section five. Section six covers the steps of the NN algorithm. Section seven narrates the process of data training, validation and mathematical expression of statistical errors. Finally, the results are analyzed and compared with other two NN models to verify the performance the proposed NN algorithm on estimating lithium-ion battery SOC.

2. Features Selection Using PCA

Input data selection is very important in constructing an optimal NN model. Irrelevant data selection not only extends the training time but also causes an increase in the estimated error. Due to a complex nonlinear characteristic of the lithium-ion battery, SOC is estimated by many features. In this research, three basic input variables including current, voltage and temperature are selected first. However, these three variables cannot estimate battery SOC precisely. Therefore, new input features must be included to the model to improve the estimation accuracy. The features will be derived from the basic variables in the form of derivative and integration. Hence, a first and second derivative of voltage $\left(dV, d^2V\right)$ and current $\left(dI, d^2I\right)$ are considered. Also, integration of current $\left(\int Idt\right)$ and voltage $\left(\int Vdt\right)$ are also taken into account. These features are selected since the sensitivity of these features is significant in estimating SOC. It is observed that the higher number inputs increases the accuracy but reduces the convergences. Hence, the correlations between input features and SOC are evaluated.

There are various methods to extract the most relevant input features such as linear correlation analysis [29], genetic algorithm [30], partial least square regression (PLSR) [31] However, each model suffers from a lack of accuracy and complex computation. Therefore, the optimal number of input variables for the estimation of SOC is computed using PCA or Karhunen Loève Transform (KLT) . PCA or KLT is a dimension reduction tool which is used to transform a large set of the dataset into a small set that still obtains the most of the information in the large dataset. PCA is a mathematical procedure which reduces the uncorrelated variables and finds a number of correlated variables that accounts for as much variability in the data as possible [32]. C. Turchetti, et al. [33] proposed KLT technique to represent the nonlinear random transformations by non-gaussian stochastic neural networks. The KLT basis set consists of the eigenvectors of the covariance matrix. The KLT is also guaranteed to provide the most efficient and accurate transformation by minimizing mean square error (MSE) in reconstruction and maximizing the entropy of the representation. This has the effect of greatly reducing the dimensionality of uncorrelated features from many variables. The similar approach can be introduced for battery charging model since the lithium-ion battery has non-linear characteristics.

The algorithm to extract feature using PCA can be explained in the following seven steps [34].

Step 1 Select the whole dataset consisting of nine variables.
Step 2 Compute mean, variance and covariance matrix.
Step 3 Calculate eigenvalues and corresponding eigenvectors of the covariance matrix.
Step 4 Extract factors based on eigenvalues greater than one.
Step 5 Select the factor which has the highest eigenvalue and highest variability.
Step 6 Calculate the eigenvector, correlations between variables and factors, and contribution of the variables (%) of the most influencing factor.
Step 7 Rank the variables based on the value of eigenvector, correlation and variable contribution from the highest to the lowest. This will arrange the variables in order of significance.

Table 1 shows the eigenvalue, variable and cumulative of three factors for data US06 at 25°C and 45°C respectively. All three factors have eigenvalues greater than one. The factor which has high eigenvalues contributes high to the explanation in the variables. The factor one contains 34% variability while the factor two and factor three capture 25% and 20% of the variance respectively at 25°C. Among three factors, factor one is chosen since it has achieved the highest value of eigenvalue and the highest variability.

Table 1. Factor analysis using PCA

Factor	F1		F2		F3	
	25°C	45°C	25°C	45°C	25°C	45°C
Eigenvalue	3.09	2.98	2.23	2.22	1.83	1.81
Variability (%)	34.43	33.15	24.82	24.69	20.38	20.12
Cumulative %	34.43	33.15	59.26	57.84	79.64	77.96

Table 2 presents the eigenvalue, correlation significance and variable contribution of each input. It is observed that current integration has the maximum eigenvector of 0.47 followed by the current, voltage integration, voltage and the first derivative of the voltage at 25°C. Similarly, at 45°C, the current integration, current, voltage integration, and voltage have a high contribution in explaining the variance. The correlation coefficient and variable contribution also prove that there are high significance and variation in current, voltage as well as their integration values where current integration holds the highest value.

Table 2. Results of PCA

Features	Eigenvectors		Correlations coefficient		Contribution of the variables (%)	
	25°C	45°C	25°C	45°C	25°C	45°C
I	0.47	0.49	0.83	0.84	22.24	24.03
V	0.41	0.39	0.71	0.68	16.45	15.60
T	-0.16	-0.12	-0.28	-0.21	2.58	1.59
dV	0.38	0.37	0.67	0.64	14.61	13.97
d^2V	-0.02	-0.11	-0.03	-0.20	0.04	1.37
dI	0.16	0.07	0.28	0.12	2.65	0.49
d^2I	-0.13	-0.17	-0.23	-0.29	1.75	2.93
$\int Idt$	0.47	0.49	0.84	0.85	22.98	24.36
$\int Vdt$	0.41	0.39	0.71	0.68	16.66	15.61

Table 3 and Table 4 show the feature selection for NN algorithm from the highest to lowest based on the values used in Table 2. Table 3 and Table 4 have the identical results for the variables ranked from one to five. However, the ranking hierarchy for the input variables placed at rank six to nine is not similar at both temperatures. These features are not considered as they are the least influential factors and they have very low correlation with the output. In summary, the first five variables are chosen out of nine variables since these five variables have the higher eigenvector, correlation and contribute almost 93% variation.

Table 3. Rank of input from highest to lowest at 25°C

Rank	1	2	3	4	5	6	7	8	9
Input	$\int Idt$	I	$\int Vdt$	V	dV	dI	T	d^2I	d^2V

Table 4. Rank of input from highest to lowest at 45°C

Rank	1	2	3	4	5	6	7	8	9
Input	$\int Idt$	I	$\int Vdt$	V	dV	d^2I	T	d^2V	dI

3. Data Collection

Battery data was collected from 18,650 $LiNiMnCoO_2$/Graphite lithium-ion cells with a nominal capacity of 2.0 Ah and voltage of 3.6 V. The upper and lower cut-off voltage of the battery is 4.2 V and 2.5 V respectively and a maximum current of 22 A. The cell was charged by constant current constant voltage (CCCV) method. The measurements were recorded in a 1-second interval. The highway driving profile named US06 [35] are used for data training and testing. Experiments were conducted at 25°C and 45°C. The current and voltage profile of US06 is shown in Fig. 1.

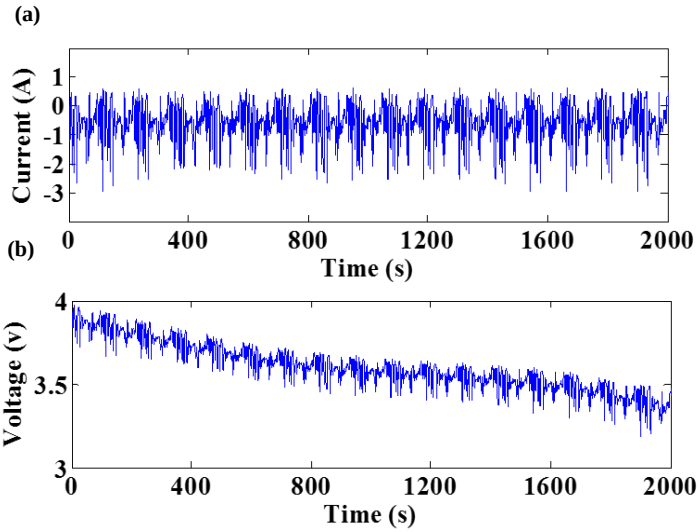

Fig. 1. US06 testing profile (a) current (b) voltage

4. Data Normalization

The training data of NN can be made more efficient and robust through appropriate normalization of data. The data normalization can enhance the convergence rate and is able to remove the negative influence. In this study, input and output are normalized to a range [-1,1] by

$$x = \frac{2\left(x - x_{\min}\right)}{x_{\max} - x_{\min}} - 1 \quad (1)$$

Where $x_{\max}$ and $x_{\min}$ are the maximum and minimum value of input vector x of the NN model. The validation dataset is scaled using the same range used in the training data.

5. Neural Network Structure

A three-layer feedforward back-propagation (BP) neural network is used in this research for the estimation of SOC. The first layer is the input layers to characterize the inputs variables, the second layer consists of one or more hidden layers and the third layer is the output layer to characterize the output variables. The input layer has inputs with weights without any processing of data. The hidden layers and output layer are called processing layer with the activation function. In NN structure, the neurons calculate the summation of the multiplying of inputs weighted with the inputs variables, and the threshold or bias. The summation is processed neurons' activation function to generate the outputs. The hidden layer uses hyperbolic tangent sigmoid function as an activation function which is defined as

$$f(x) = \frac{1}{\left(1+e^{-x}\right)} \tag{2}$$

The output layer can be mathematically represented as

$$Y = f\left(\sum_{j=1}^{N} w_j X_j + b_j\right) \tag{3}$$

Where X and Y represent the input and the output variables of the BPNN model, respectively, w_j is the weight, b_j represents the bias.

The weights and biases values are estimated in each neuron is a supervised training process with the learning data. During the training process, NN minimizes the error rate between estimated SOC and actual SOC by adjusting the weights and biases at each iteration. The training process stops once the distinction is lower than the present value of the error rate. Fig. 2 shows the NN structure with optimal inputs.

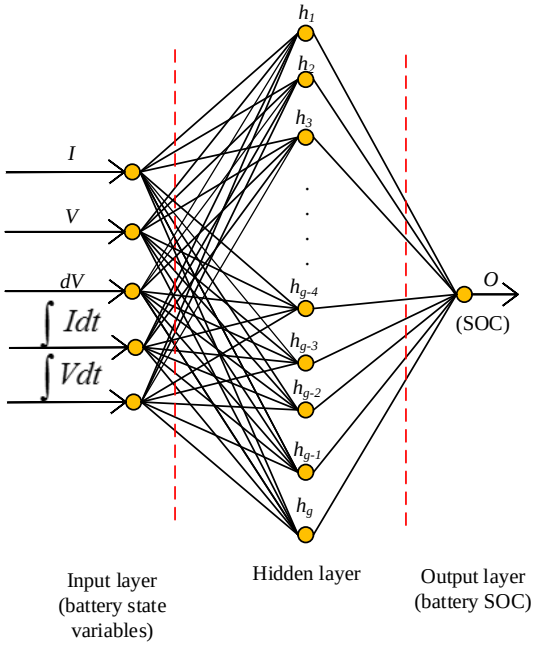

Fig. 2. Structure of NN with optimal input variables

6. Optimal NN Algorithm

The flowchart of optimal NN algorithm is shown in Fig. 3

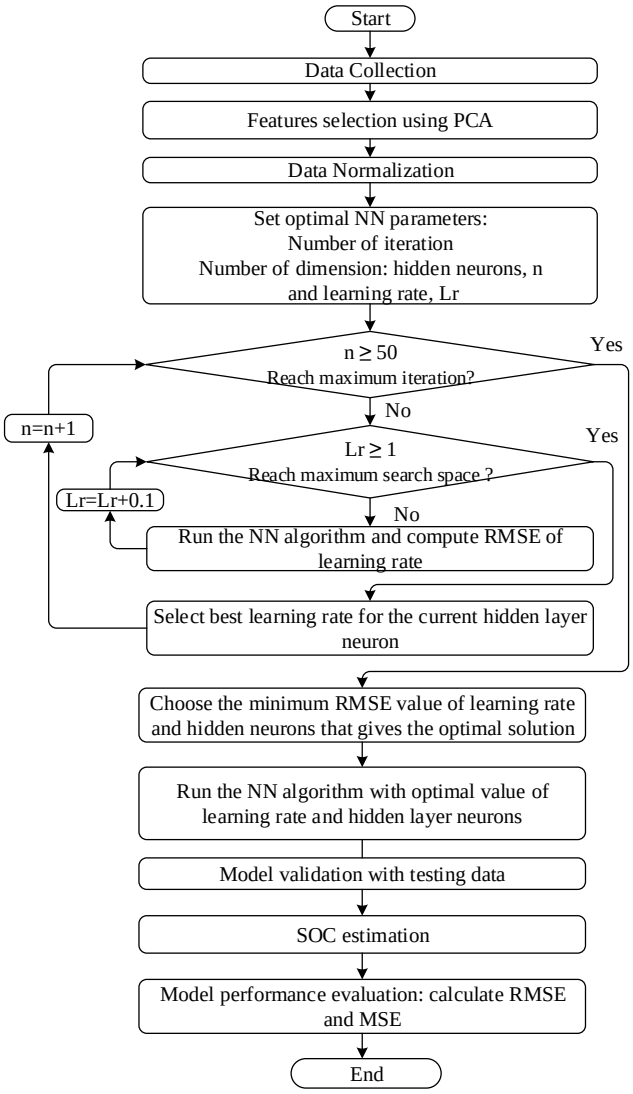

Fig. 3. Proposed optimal NN algorithm flowchart for SOC estimation

The steps of the proposed NN algorithm for estimating SOC are described as follows.

Step 1 The estimation process starts by selecting the appropriate inputs. In this study, five inputs are selected out of many variables including $I, V, dV, \int Idt, \int Vdt$ since these five inputs have a significant relationship with battery SOC which is mentioned in section three.

Step 2 The input and output data are normalized to a range [-1,1].

Step 3 The maximum iteration is selected as 50. The initial number of the hidden neuron and learning rate assign as 1 and 0.1 respectively.

Step 4 A 'for loops' is introduced to handle all the

numbers of neurons in the search space.

Step 5 At the same time, another 'for loops' is initiated inside the previous 'for loops' to find an optimal value of learning rate. During each iteration, the objective function (i.e., RMSE) is calculated for the current hidden layer neuron. The search space is controlled for 1 as the maximum values. The value of learning rate is increased by 0.1 and will stop until it reaches maximum search space.

Step 6 The learning rate is chosen for the current hidden layer neuron.

Step 7 The minimum value of the objective function for hidden layer and learning rate are selected to achieve the best results accuracy.

Step 8 The simulation is executed with the activation function of the NN algorithm with the optimal number of neurons and learning rate that has achieved from the previous sequences.

Step 9 The model is verified using testing data.

Step 10 SOC is estimated and compared the results with actual SOC.

Step 11 Evaluate the performance of the proposed model by estimating RMSE and MSE.

7. Model Training and Validation

US06 is randomly divided into two data sets. The model is trained by using 60% randomly selected data and verified by using 40% randomly selected data. Training of the NN is performed using Levenberg-Marquardt back propagation because it has good training speed and maintains very good accuracy. In this study, the maximum number of epochs is 1000 and the performance goal is set as 0.000001.

Two statistical error terms are used to evaluate the results of the proposed NN model including RMSE and MSE. The mathematical expression of RMSE and MSE are expressed as follows:

$$RMSE = \sqrt{\frac{1}{N}\sum_{i=1}^{N}\left(I_{es} - I_a\right)^2} \quad (4)$$

$$MSE = \frac{1}{N}\sum_{i=1}^{N}\left(I_{es} - I_a\right)^2 \quad (5)$$

Where I_{es} represents the estimated value, I_a is actual value and N is a number of observations.

8. Results and Discussion

This study presents three NN models to estimate SOC based on different input variables, hidden layer and learning rate. The NN1 model takes current (I), voltage (V), temperature (T) as inputs. The number of hidden neurons is considered as 10 and learning rate is 0.5. The inputs of the NN2 model are current (I), voltage (V), temperature (T), the first derivative of voltage and current (dI, dV). The hidden neuron and learning rate is chosen as 15 and 0.8 respectively. The NN3 model optimizes the number of inputs, hidden layer and learning rate. Three NN models estimate SOC using a three-layer structure with Levenberg-Marquardt back propagation training and the same activation function.

8.1 NN1 model

Fig. 4 compares the estimated SOC with actual SOC for the NN1 model at 25°C and 45°C. The solid curve represents the SOC estimated by coulomb counting method. It is observed that both show similar characteristics to predict SOC. However, SOC estimated at 45°C is more stable than that of 25°C. Ambient temperature has a significant effect on battery SOC. The increment of ambient temperature results in an increase in battery capacity [36]. This is due to the fact that the temperature acceleration results in a reduction in viscosity and a rise in activity of the electrolyte which may support the migration impact and ion diffusion [37].

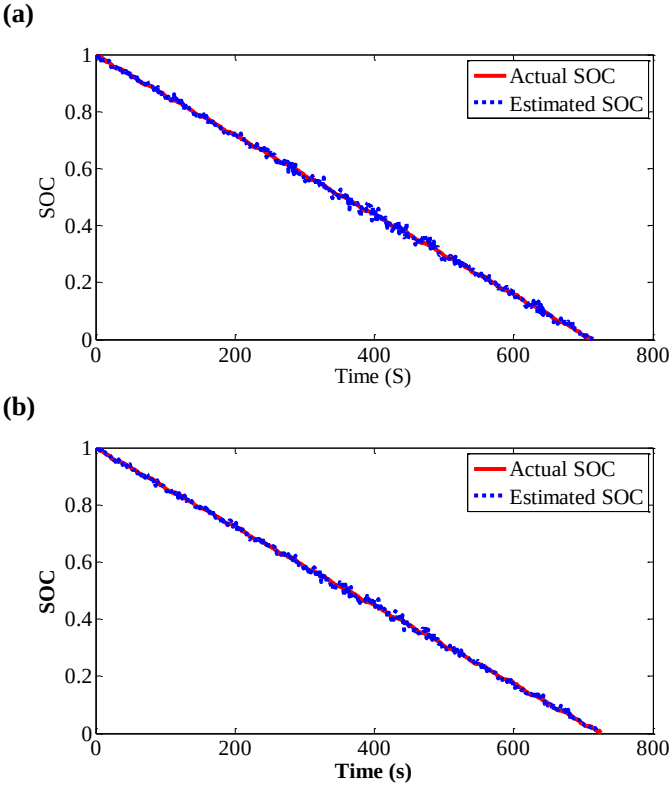

Fig. 4. SOC estimation of NN1 model (a) 25°C (b) 45°C

8.2 NN2 model

Likewise, for the NN2 model, the SOC estimation performs better when it is tested at 45°C as shown in Fig. 5. In addition, the performance is enhanced compared to NN1 model due to the increasing number of input features and different values of hidden layer neurons and learning rate. The results demonstrate that there is an improvement in SOC estimation when the number of input variables is increased. However, it does not mean that the more we have the input features, the less we achieve error in SOC estimation. Selecting input features needs careful observations since increasing the input features can cause model complexity and lengthen the training time. Similarly, if the hidden neuron and learning rate are not optimized, then the estimation error will also increase.

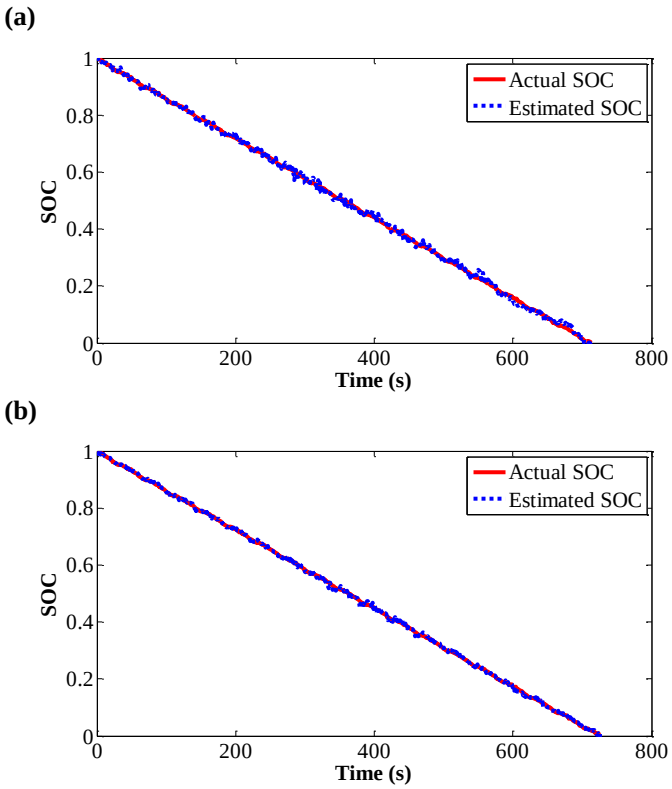

Fig. 5. SOC estimation of NN2 model (a) 25°C (b) 45°C

8.3 NN3 Model

The NN3 model is the proposed model with the optimal number of input features together with an optimal number of hidden neurons and learning rate. The proposed NN model computes the optimal number of neurons and hidden layer based on RMSE. Fig. 6 (a) shows that the RMSE is very high at the beginning part of neurons for the US06 cycle at 25°C. The highest value of RMSE is estimated at 0.018 when the number of a neuron is one and since then, RMSE starts decreasing and achieves the lowest RMSE of 0.0057 with 22 neurons. The value of RMSE starts rising with some quick fluctuations between neurons 10 and 50. The result indicates that increasing the number neurons does not attain a better performance. Fig. 6 (b) shows the RMSE value of a number of neurons for US06 cycles at 45°C. Similarly, the higher value of RMSE is achieved at the initial part of neurons. There is a dramatic decrease in RMSE value for neurons placed from one to three. The RMSE starts declining again and reaches its lowest value of 0.0033 with 25 hidden neurons. The value of RMSE fluctuates between the value of 0.003 and 0.005 when the neuron value lies between 10 and 50 which again proves that the model is not suitable for higher values of neurons. The learning rate is computed as 0.1 for both 25°C and 45°C.

Fig. 7 shows the simulation results of SOC estimation for the proposed NN model. The estimated SOC is nearly aligned with actual SOC which proves the high accuracy of the proposed model compared to the first and second NN model.

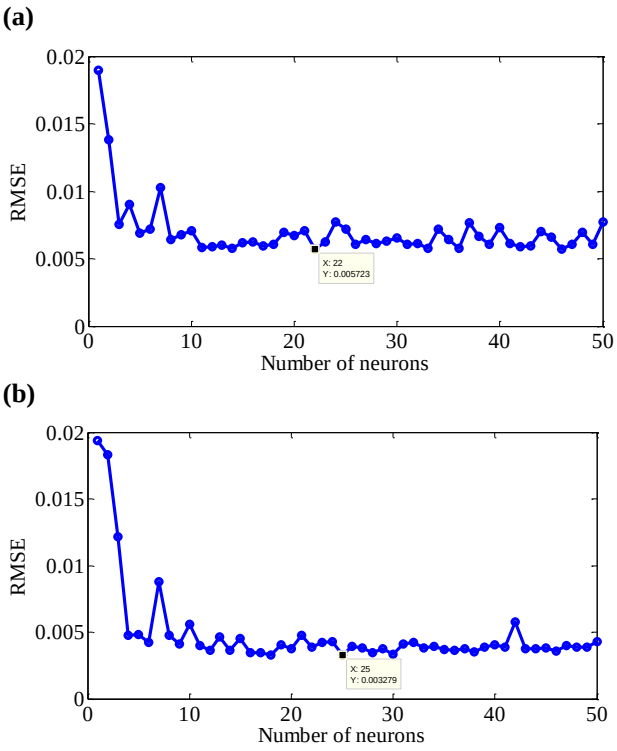

Fig. 6. Proposed NN model training RMSE vs number of neurons (a) 25°C (b) 45°C

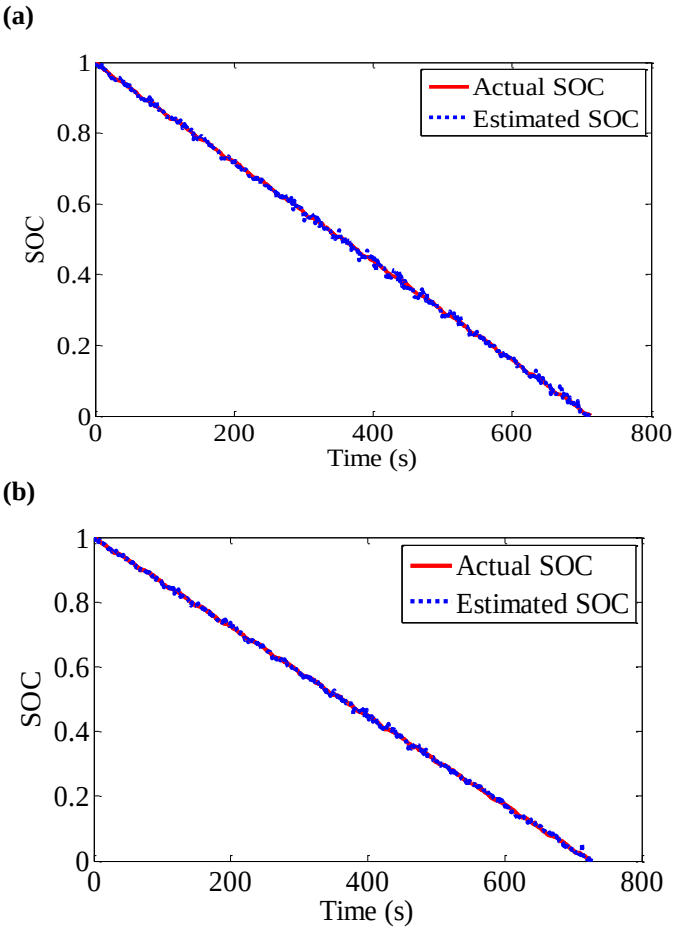

Fig. 7. SOC estimation of the proposed model (a) 25°C (b) 45°C

Fig. 08 shows the absolute error which is the difference between actual SOC and estimated SOC. The range of absolute error lies at between -2% and +2% at 25°C with rapid fluctuations. Nevertheless, at 45°C, absolute error is more stable and has less fluctuation than operating at 25°C. The majority error lies at between -1% and +1% with a very few values reach -2% and +2%.

(a)

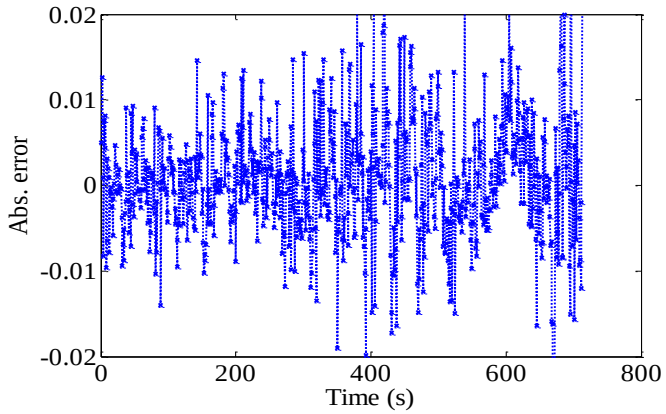

(b)

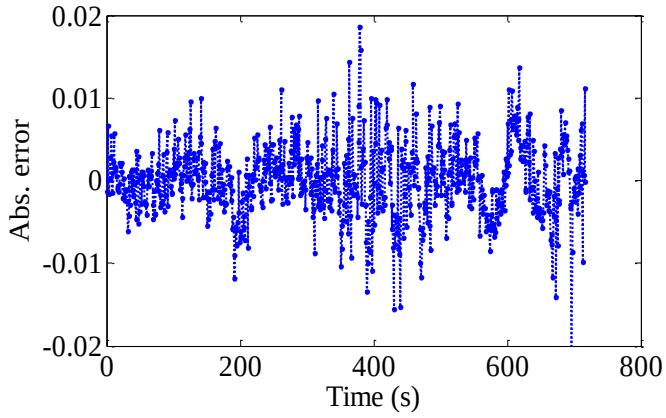

Fig. 8. Absolute error of the proposed model (a) 25°C (b) 45°C

8.4 Comparative Analysis

Fig. 9 and Fig. 10 compares the performance among three NN models based on MSE and RMSE. The RMSE for the NN1 and NN2 models are estimated as 0.86% and 0.82% respectively at 25°C while the proposed model has an RMSE of 0.64% which is a 26% and 22% reduction from the NN1 model and NN2 model. The MSE value of the proposed NN model is also decreased and dropped by 45% and 39% compared to the NN1 and NN2 model. The value RMSE and MSE for the NN1 and NN2 models are declined further at 45°C and reach at 0.65% and 0.47% respectively. However, the proposed model performs better and achieves RMSE of 0.42% which is a decrement by 35% and 11% compared to NN1 and NN2 model respectively. There is also an improvement of MSE in the proposed NN model where the error is reduced by 57% and 18% in comparison to the NN1 model and NN2 model.

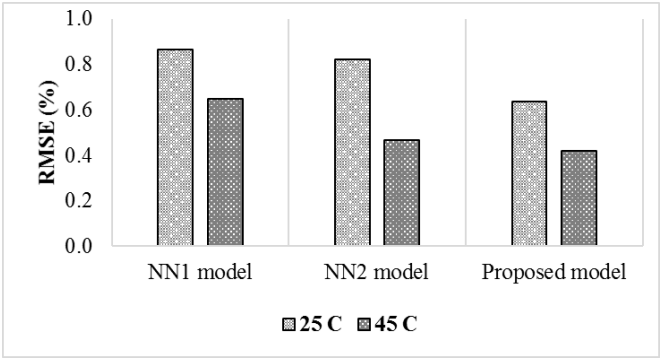

Fig. 9. RMSE comparison of three NN models

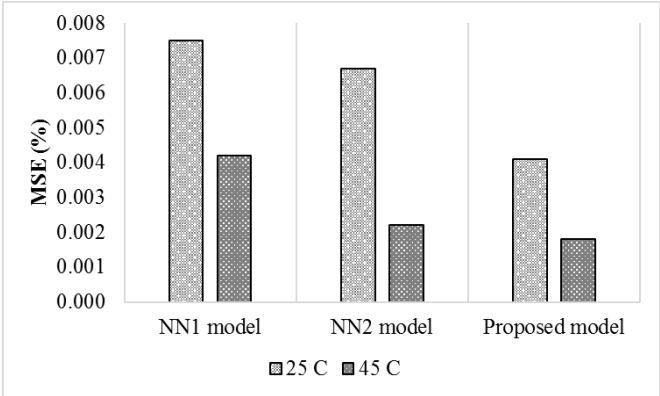

Fig. 10. MSE comparison of three NN models

9. Conclusion

An advanced NN model with an optimal value of inputs, hidden layer and learning rate are presented in this paper. The detailed explanation of PCA algorithm, NN operating principle, and the optimal algorithm have been provided. US06 cycle is used for model training and validation at two different temperatures. The proposed model is compared with two different NN models to prove the model robustness and accuracy. The results are significant to conclude that:

- Selecting the most relevant input features is an effective method to optimize the NN model. The study considers many input variables including current, voltage, temperature with their first, second derivative as well as integration. However, the results obtained from PCA demonstrate that the combination of five inputs including $I, V, dV, \int Idt, \int Vdt$ have strong relevance with battery SOC.
- Finding the optimal number of hidden neurons and learning rate is another promising method to enhance the SOC accuracy. The optimal number hidden layer neurons are computed as 22 and 25 based on lowest RMSE at 25°C and 45°C respectively. The results also show that increasing the number hidden layer neuron does not improve model performance. The learning rate is 0.1 at both temperatures. The validation reports prove that the proposed model is effective in enhancing accuracy and has RMSE under 1%.

- A comparison is studied between the proposed model and two different NN models to check the model accuracy and robustness. The proposed NN model is demonstrated as a better model in terms of performance and accuracy. The results show that there is a reduction in RMSE by 26% and 22% and MSE by 45% and 39% respectively compared to the NN1 model and NN2 model at 25°C.

Acknowledgement

The authors gratefully acknowledge Universiti Kebangsaan Malaysia for the financial funding under research grant DIP-2015-012.

References

[1] M. A. Hannan, M. S. H. Lipu, A. Hussain, and A. Mohamed, "A review of lithium-ion battery state of charge estimation and management system in electric vehicle applications: Challenges and recommendations," Renew Sustain Energy Rev, vol. 78, pp. 834–854, 2017.

[2] J. Y. Yong, V. K. Ramachandaramurthy, K. M. Tan, and N. Mithulananthan, "A review on the state-of-the-art technologies of electric vehicle, its impacts and prospects," Renew Sustain Energy Rev, vol. 49, pp. 365–385, 2015.

[3] S. N. Tsotoulidis and A. N. Safacas, "Analysis of a Drive System in a Fuel Cell and Battery powered Electric Vehicle," Int J Renew Energy Res, vol. 1, no. 3, pp. 140–151, Oct. 2011.

[4] H. Turker, "Design optimization ofan interior permanent magnet synchronous machine (IPMSM) for electric vehicle application," in 2016 IEEE International Conference on Renewable Energy Research and Applications (ICRERA), 2016, pp. 1034–1038.

[5] Z. Cerovsky and P. Mindl, "Impact of Energy Production Technology on gas emission by Electric Hybrid and Electric Vehicles," Int J Renew Energy Res, vol. 1, no. 3, pp. 118–125, Oct. 2011.

[6] M. A. Hannan, F. A. Azidin, and A. Mohamed, "Hybrid electric vehicles and their challenges: A review," Renew Sustain Energy Rev, vol. 29, pp. 135–150, 2014.

[7] H. Turker, "Review of electric motors for grid connected integrated battery chargers in electric vehicle applications," in 2016 IEEE International Conference on Renewable Energy Research and Applications (ICRERA), 2016, pp. 1029–1033.

[8] A. Fotouhi, D. J. Auger, T. Cleaver, N. Shateri, K. Propp, and S. Longo, "Influence of battery capacity on performance of an electric vehicle fleet," in 2016 IEEE International Conference on Renewable Energy Research and Applications (ICRERA), 2016, pp. 928–933.

[9] Z. Chen, B. Xia, C. You, and C. C. Mi, "A novel energy management method for series plug-in hybrid electric vehicles," Appl Energy, vol. 145, pp. 172–179, 2015.

[10] Y. Nakanishi, T. Honda, K. Kasamura, Y. Nakashima, K. Nakano, K. Kondo, and H. Higaki, "Bio-inspired shaft seal in coolant pump for electric vehicles," in 2016 IEEE International Conference on Renewable Energy Research and Applications (ICRERA), 2016, pp. 112–117.

[11] M. A. Hannan, M. M. Hoque, A. Mohamed, and A. Ayob, "Review of energy storage systems for electric vehicle applications: Issues and challenges," Renew Sustain Energy Rev, vol. 69, pp. 771–789, 2017.

[12] M. A. Hannan, M. M. Hoque, S. E. Peng, and M. N. Uddin, "Lithium-Ion Battery Charge Equalization Algorithm for Electric Vehicle Applications," IEEE Trans Ind Appl, pp. 1–1, 2017.

[13] A. Fotouhi, D. J. Auger, K. Propp, S. Longo, and M. Wild, "A review on electric vehicle battery modelling: From Lithium-ion toward Lithium–Sulphur," Renew Sustain Energy Rev, vol. 56, pp. 1008–1021, 2016.

[14] S. Manzetti and F. Mariasiu, "Electric vehicle battery technologies: From present state to future systems," Renew Sustain Energy Rev, vol. 51, pp. 1004–1012, 2015.

[15] S. C. Chen, C. C. Wan, and Y. Y. Wang, "Thermal analysis of lithium-ion batteries," J Power Sources, vol. 140, no. 1, pp. 111–124, 2005.

[16] M. M. Hoque, M. A. Hannan, and A. Mohamed, "Voltage equalization control algorithm for monitoring and balancing of series connected lithium-ion battery," J Renew Sustain Energy, vol. 8, no. 2, p. 25703, Mar. 2016.

[17] J. Speirs, M. Contestabile, Y. Houari, and R. Gross, "The future of lithium availability for electric vehicle batteries," Renew Sustain Energy Rev, vol. 35, pp. 183–193, 2014.

[18] K. Uddin, S. Perera, W. Widanage, L. Somerville, and J. Marco, "Characterising Lithium-Ion Battery Degradation through the Identification and Tracking of Electrochemical Battery Model Parameters," Batteries, vol. 2, no. 2, p. 13, 2016.

[19] A. El Mejdoubi, A. Oukaour, H. Chaoui, H. Gualous, J. Sabor, and Y. Slamani, "State-of-Charge and State-of-Health Lithium-Ion Batteries' Diagnosis According to Surface Temperature Variation," IEEE Trans Ind Electron, vol. 63, no. 4, pp. 2391–2402, Apr. 2016.

[20] M. Dubarry, B. Y. Liaw, M.-S. Chen, S.-S. Chyan, K.-C. Han, W.-T. Sie, and S.-H. Wu, "Identifying battery aging mechanisms in large format Li ion cells," J Power Sources, vol. 196, no. 7, pp. 3420–3425, 2011.

[21] T. Utsunomiya, O. Hatozaki, N. Yoshimoto, M. Egashira, and M. Morita, "Influence of particle size on the self-discharge behavior of graphite electrodes in lithium-ion batteries," J Power Sources, vol. 196, no. 20, pp. 8675–8682, 2011.

[22] Y. Zhang, W. Song, S. Lin, and Z. Feng, "A novel model of the initial state of charge estimation for LiFePO 4 batteries," J Power Sources, vol. 248, pp. 1028–1033, 2014.

[23] L. Zheng, L. Zhang, J. Zhu, G. Wang, and J. Jiang, "Co-estimation of state-of-charge, capacity and resistance for lithium-ion batteries based on a high-fidelity electrochemical model," Appl Energy, vol. 180, pp. 424–434, 2016.

[24] K. Lim, H. A. Bastawrous, V.-H. Duong, K. W. See, P. Zhang, and S. X. Dou, "Fading Kalman filter-based real-

time state of charge estimation in LiFePO4 battery-powered electric vehicles," Appl Energy, vol. 169, pp. 40–48, 2016.
[25] A. Benyamina, S. Moulahoum, I. Colak, and R. Bayindir, "Hybrid fuzzy logic-artificial neural network controller for shunt active power filter," in 2016 IEEE International Conference on Renewable Energy Research and Applications (ICRERA), 2016, pp. 837–844.
[26] S. G. Li, S. M. Sharkh, F. C. Walsh, and C. N. Zhang, "Energy and Battery Management of a Plug-In Series Hybrid Electric Vehicle Using Fuzzy Logic," IEEE Trans Veh Technol, vol. 60, no. 8, pp. 3571–3585, Oct. 2011.
[27] D. H. K. B and S. K. Matam, "Operating Reserve forecasting in a wind integrated power system using Hybrid Support Vector Machine-Fuzzy Inference System," Int J Renew Energy Res, vol. 7, no. 2, pp. 531–539, Jun. 2017.
[28] J. C. Alvarez Anton, P. J. Garcia Nieto, C. Blanco Viejo, and J. A. Vilan Vilan, "Support Vector Machines Used to Estimate the Battery State of Charge," IEEE Trans Power Electron, vol. 28, no. 12, pp. 5919–5926, Dec. 2013.
[29] W. Sun, M. Ye, and Y. Xu, "Study of carbon dioxide emissions prediction in Hebei province, China using a BPNN based on GA," J Renew Sustain Energy, vol. 8, no. 4, p. 43101, Jul. 2016.
[30] K. Nag and N. R. Pal, "A Multiobjective Genetic Programming-Based Ensemble for Simultaneous Feature Selection and Classification," IEEE Trans Cybern, vol. 46, no. 2, pp. 499–510, Feb. 2016.
[31] C. Bo, B. Zhifeng, and C. Binggang, "State of charge estimation based on evolutionary neural network," Energy Convers Manag, vol. 49, no. 10, pp. 2788–2794, Oct. 2008.
[32] Q. Jiang, X. Yan, and B. Huang, "Performance-Driven Distributed PCA Process Monitoring Based on Fault-Relevant Variable Selection and Bayesian Inference," IEEE Trans Ind Electron, vol. 63, no. 1, pp. 377–386, Jan. 2016.
[33] C. Turchetti, P. Crippa, M. Pirani, and G. Biagetti, "Representation of Nonlinear Random Transformations by Non-Gaussian Stochastic Neural Networks," IEEE Trans Neural Networks, vol. 19, no. 6, pp. 1033–1060, Jun. 2008.
[34] A. Tharwat, "Principal component analysis - a tutorial," Int J Appl Pattern Recognit, vol. 3, no. 3, p. 197, 2016.
[35] F. Zheng, Y. Xing, J. Jiang, B. Sun, J. Kim, and M. Pecht, "Influence of different open circuit voltage tests on state of charge online estimation for lithium-ion batteries," Appl Energy, vol. 183, pp. 513–525, 2016.
[36] S. S. Zhang, K. Xu, and T. R. Jow, "Electrochemical impedance study on the low temperature of Li-ion batteries," Electrochim Acta, vol. 49, no. 7, pp. 1057–1061, 2004.
[37] D. H. Doughty, E. P. Roth, C. C. Crafts, G. Nagasubramanian, G. Henriksen, and K. Amine, "Effects of additives on thermal stability of Li ion cells," J Power Sources, vol. 146, no. 1–2, pp. 116–120, 2005.